Electrospray Ionization Mass Spectrometry and Hydrogen/Deuterium Exchange for Probing the Interaction of Calmodulin with Calcium

Olga Nemirovskiy, Daryl E. Giblin, and Michael L. Gross
Department of Chemistry, Washington University, St. Louis, Missouri, USA

The extent of H/D exchange of the protein calmodulin in solution was monitored by mass spectrometry following electrospray ionization (ESI) of the protein. In the absence of Ca^{2+}, approximately 115 protons are exchanged for deuteriums after 60 min. As the calmodulin is titrated with Ca^{2+}, the extent of exchange decreases significantly (i.e., by 24 protons), indicating Ca^{2+}-induced folding of the protein to a tighter, less solvent-accessible form. The extent of H/D exchange ceases to decrease when the amount of added Ca^{2+} is sufficient to convert greater than 80% of the calmodulin to a form bound by four calcium ions. Lysozyme, a protein of similar molecular weight, does not show a significant decrease in the extent of H/D exchange as it binds to Ca^{2+}, indicating that the changes in H/D exchange for calmodulin reflect tertiary structural change that occur upon binding with Ca^{2+}. (J Am Soc Mass Spectrom 1999, 10, 711–718) © 1999 American Society for Mass Spectrometry

Electrospray ionization (ESI) coupled with mass spectrometry (MS) provides, in addition to molecular weight, important information on the structure of proteins [1]. For example, the extent of charging and the resultant distribution of molecular ions depend on conformation, solvent accessibility of various sites, and effective pK values of the acidic and basic functional groups on the side chains [2]. For many proteins, there is a correlation between the maximum number of charges and the number of basic amino-acid residues [2–5]. For example, the maximum charge state observed in the ESI mass spectrum of bovine ubiquitin corresponds to the 13 basic residues that are available for protonation.

The maximum of a charge-state distribution depends on the conformation of the biomolecule in solution [2–5]. Often when a protein is in a native conformation, a narrow charge-state distribution centered at a high mass-to-charge ratio (low charge states) pertains. Upon denaturation, the protein conformation becomes more open, undergoing a greater extent of charging and a shift of the charge-state distribution to the lower mass-to-charge (m/z) ratios.

Heat-induced conformational changes in proteins also lead to alterations of charge-state distributions [6–8]. Increasing the temperature of the ESI interface induces denaturation of proteins, leading to a shift in the charge distribution to higher charge states (lower m/z).

Address reprint requests to Michael L. Gross, Department of Chemistry, Box 1134, Washington University, One Brookings Drive, St. Louis, MO 63130. E-mail: mgross@wuchem.wustl.edu

Although charge-state distributions give some information on three-dimensional structure, a more detailed view can be achieved by hydrogen/deuterium (H/D) exchange experiments, which can be monitored by ESI-MS [2, 9–13]. Proteins with open structures have amide hydrogens that are more accessible to the solvent (D_2O), and their exchange will proceed at higher rates and to a greater extent. Native, tightly folded proteins have fewer accessible amide hydrogens, leading to a lower uptake of deuterium.

NMR has been the "gold standard" for measuring hydrogen/deuterium exchange of proteins and identifying intermediates in protein folding [14–17]. NMR monitors the average exchange at individual sites over the distribution of protein molecules, permitting interpretation of the measured proton occupancies in the 3D structure. Information on different populations of protein molecules, however, cannot be readily obtained by NMR methods. Approximate molecular-weight limits for H/D exchange by NMR are: 15 kDa (routine), 15–30 kDa (more difficult but feasible), and 30–50 kDa (possible in selected cases). The main limitation for large proteins is establishing sequence-specific NMR resonance assignments. Without assignments, an amide exchange can still be monitored, but without site-specificity. NMR is nondestructive, and the sample can be fully recovered. The measurements are made for molecules in the solution state; thus, there is no concern about perturbing solution equilibria as there may be when samples are taken from solution into the gas phase, as is required by ESI-MS.

For H/D exchange, MS has advantages over NMR

1044-0305/99/$20.00
PII S1044-0305(99)00036-7

Received November 18, 1998
Revised March 15, 1999
Accepted March 31, 1999

with respect to the sensitivity and molecular-weight considerations. For the H/D exchange experiments by NMR, 0.5 mL of a 0.5–1.5 mM solution is necessary, whereas MS can be used in the micromolar concentration range although a number of solutions must be prepared if kinetics are to be measured or titrations conducted. MS can work with higher mass protein than can NMR, and analyses are rapid. Although MS can measure the most rapidly exchanging amide hydrogens and NMR typically cannot, the simplicity of the data interpretation for H/D exchange measurements is approximately the same for both NMR and MS.

H/D exchange and ESI/MS cannot directly provide information on the location of hindered or exposed amide hydrogens, but digestion of a labeled protein in its folded state and further investigation of the peptide fragments by ESI-MS can identify sites of slow and rapid exchange [18–20]. This procedure coupled with tandem mass spectrometry of the labeled peptide segments may ultimately allow the accurate location of exchangeable sites. Despite its advantages, the use of MS for H/D exchange is in its infancy, and more efforts are required to validate its accuracy.

We chose the protein calmodulin to evaluate the capability of ESI and MS to follow an interaction in which metal–ion binding causes changes in the conformation of the protein. The calcium ion can be viewed as a messenger, and upon Ca^{2+} binding, calmodulin binds to target enzymes and related small molecules. Examples are the interactions of Ca^{2+}-loaded calmodulin with small hydrophobic drugs [21], naturally occurring peptides [22], and some enzymes [23]. The upshot of these many studies is that calcium binding to calmodulin is cooperative with respect to its two globular domains and promotes a conformational change that exposes a hydrophobic surface that is necessary for binding to target enzymes. The affinity of the calcium-loaded calmodulin to the targets can be seven orders of magnitude greater than that of the apocalmodulin.

X-ray crystallographic studies of Ca^{2+} binding proteins show that they possess a common helix–loop–helix (EF-hand) structural domain in their metal-binding sites. Although the X-ray structure of CaM-4Ca (where CaM is calmodulin) has been determined, there is no crystallographic determination of the apo-CaM because suitable apocalmodulin crystals have not yet been prepared. Nevertheless, NMR [24–27] was used to obtain solution structures, and they suggest that each domain of CaM-4Ca in solution has a greater surface area, less flexibility, and a greater average separation relative to apo-CaM.

The lack of direct X-ray crystallography data and the success of our previous investigation of calmodulin, in which we demonstrated the capability of ESI to detect binding of Ca^{2+}-bound calmodulin to hydrophobic peptides [28], have motivated us to examine the effect of Ca^{2+} binding on the folding of calmodulin by mass spectrometry. Additional incentive comes from the realization that the use of NMR to monitor H/D exchange of the calcium-induced folding of calmodulin has not been reported to our knowledge.

A final incentive is that we wish to develop an alternate approach using ESI-MS to study peptide–ligand interactions such as the binding of Ca^{2+} to CaM and the induced conformational changes in the protein. Moreover, some controversy has arisen over the structure adopted by CaM-4Ca as determined by X-ray diffraction [29–31], small-angle X-ray scattering [32, 33], NMR [34–39], gel-permeation chromatography [40–42], and lifetime-resolved fluorescence resonance energy transfer [43] studies.

Experimental

Materials

Porcine calmodulin MW 16792 Da was obtained from Ocean Biologics Co. (Edmonds, WA), and hen egg lysozyme was obtained from Sigma (St. Louis, MO).

ESI-Mass Spectrometry

ESI mass spectra were recorded by using a prototype VG ZAB-T four-sector tandem mass spectrometer [44] equipped with a VG electrospray source (Micromass, Manchester, UK). A Harvard Model 22 syringe pump (Harvard Apparatus, South Natick, MA) was used to infuse a solution of 90/9/1 water/methanol/formic acid to the spray needle at a rate of 10 μL/min. Samples incubated for various time periods were introduced into the solution via a 20-μL loop Rheodyne 7125 valve. The spray needle was maintained at 8000 V, and the counter electrode (pepper pot) potential was 5000 V. The sampling cone, skimmer lens, skimmer, hexapole, and ring electrode were 4200, 4160, 4160, 4150, and 4120 V, respectively. Nitrogen was used separately as both bath and nebulizer gas with flow rates of 400 and 12 L/h, respectively (the latter was the acceleration voltage). The bath-gas temperature was maintained at 50 °C. The mass spectrometer was calibrated from *m/z* 600 to 2600 by using a solution of CsI. All experiments made use of only the first two sectors and were done with a mass resolving power of 1300 (10% valley definition) and a scan speed of 15 s/decade. Ten scans were signal averaged and processed by using the VG Opus operating system realized on a DEC-alpha workstation. The raw ESI spectra were transformed by using a maximum entropy algorithm (MaxEnt) obtained from Micromass.

H/D Exchange Protocol

For H/D exchange of apocalmodulin, 1 mg of the protein was dissolved in 400 μL of 20 mM ammonium acetate buffer (pH 7, adjusted with ammonium hydroxide), and a 10-μL aliquot was taken to determine the extent of H/D exchange at a given time point in the rate study. The exchange was initiated at room temperature and pH 7 by mixing the 10-μL aliquot with 90 μL of D_2O (Cambridge Isotope Laboratories, Andover, MA)

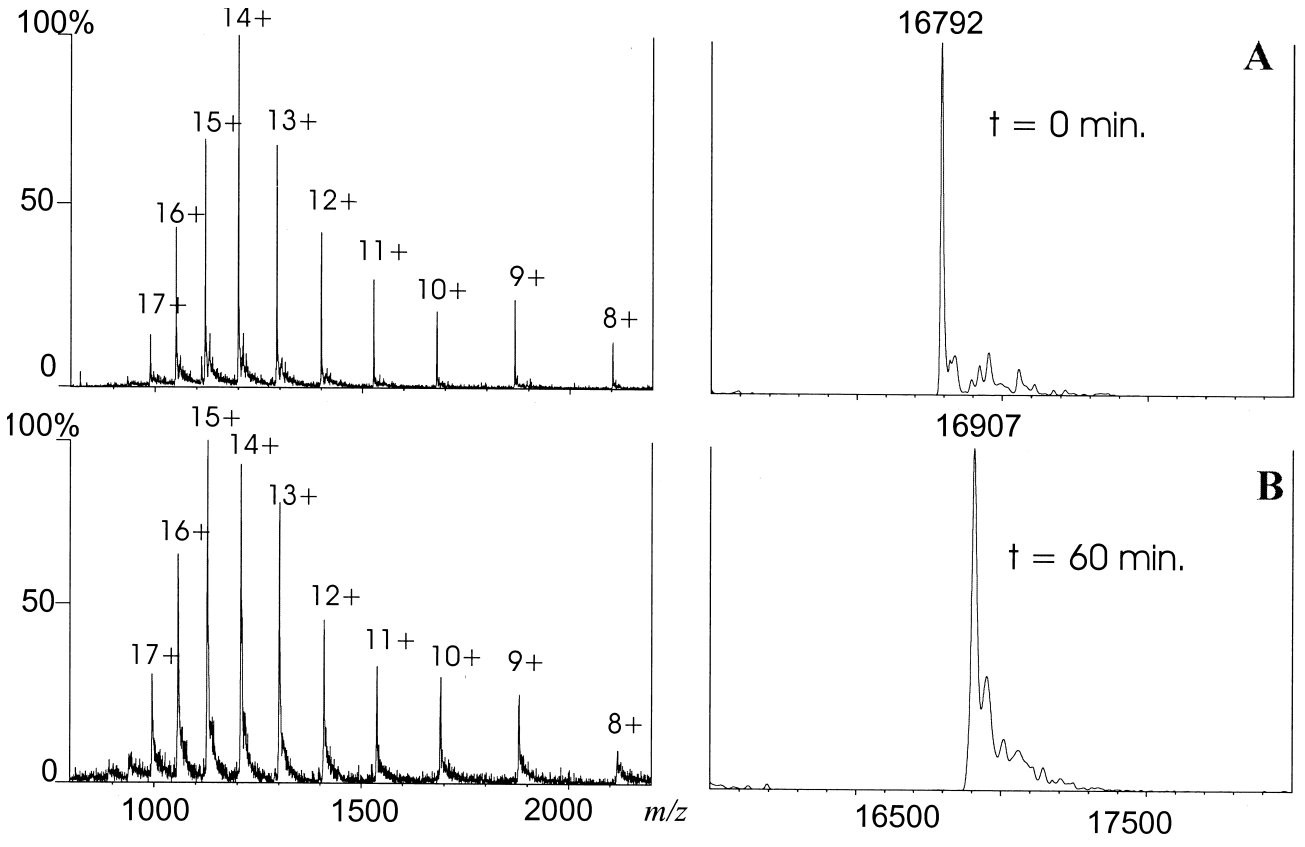

Figure 1. Typical ESI mass spectra of apocalmodulin after 0 and 60 min of H/D exchange. Note the increase in mass, indicating exchange of 115 protons for deuterons.

to give a protein concentration of 15 μM. After an exchange period, which varied from 30 s to 24 h, the exchange was quenched by adding 300 μL of ice-cold, 90/9/1 water/methanol/formic acid solution (pH 2.5). Under these conditions of pH and temperature, the rate constants for exchange are reduced by 4–5 orders of magnitude [45]. A 20-μL aliquot with a final protein concentration of 4 pmol/mL was loop-injected at quench times that varied from 0 to 30 min for ESI-MS analysis. The procedure was repeated to obtain the time-dependent curve.

For the H/D exchange experiments of metal-loaded calmodulin, 100 μL of 150-μM protein solution was added to 100 μL of calcium acetate at various concentrations: 0.01, 0.02, 0.04, 0.09, 0.16, 0.25, 0.36, 0.49, 0.64, 0.81, and 1.0 mM (concentration of salt in exchange media). A 20-μL aliquot was withdrawn to measure the extent of H/D exchange at 60 min (a time when exchange was relatively constant). The measurement of H/D exchange for Ca^{2+}-bound CaM was performed at room temperature and pH 7. Because the protein denatures and releases calcium ions bound to it during the quench event, it was the molecular weight of apocalmodulin that was recorded to give the number of deuteriums exchanged. Exchange-rate curves for calmodulin were obtained at 0.04 and 0.49 mM Ca^{2+} concentrations. For binding of CaM to magnesium, only one point at 0.49 mM Mg^{2+} after 60 min of exchange was obtained. For lysozyme, the H/D exchange kinetics curves were obtained both in the absence of metal and in 0.49 mM calcium acetate.

Results and Discussion

H/D Exchange Experiments

To examine the effect of Ca^{2+} binding on calmodulin folding, we submitted the apocalmodulin and holocalmodulin, which was formed in a titration with Ca^{2+}, to H/D exchange and recorded the results with ESI-MS. The deuterium-exchange experiment was in the "forward" direction; that is, the protein at various points in the titration was equilibrated in D_2O as a function of time. The difference in the molecular weights of deuterated and undeuterated calmodulin provides the average number of amide protons that exchanged with deuterons (typical data are in Figure 1). Because the difference is of the greatest interest, for every H/D exchange experiment, a control experiment was conducted in which samples were not incubated in D_2O.

Apocalmodulin exchanged 125 amide (backbone) protons for deuterons in 85% D_2O/15% H_2O, pH 7 during 24 h as determined by its increase in mass. The extent of deuterium incorporation is 84% of the total available amide hydrogens. Side chains containing functional groups undergo facile H/D exchange and are not counted because they are presumably rapidly

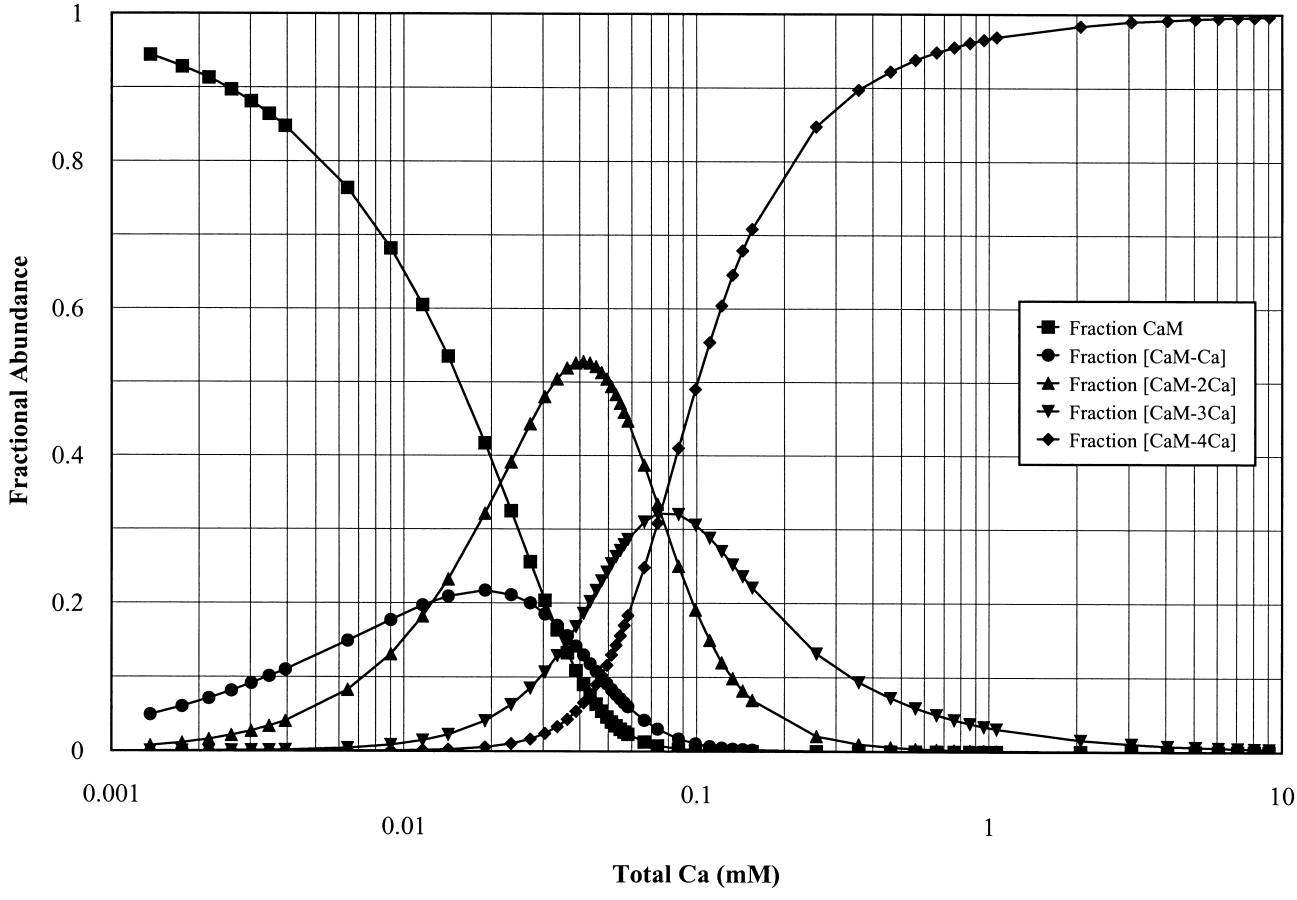

Figure 2. Fractional species calculation for Ca_x^{2+} (calmodulin) as a function of $[Ca^{2+}]$. The total calmodulin concentration is 15 μM.

back-exchanged during the quench event that precedes the MS measurement [45].

The effect of quench time on the number of exchanged backbone hydrogens was evaluated by varying the quench time from 0 to 30 min (for quench time of 0 min, there is a 2-min delay from quench to introduction into the mass spectrometer). An increase in the back exchange of only two hydrogens (error is ± 1 hydrogen) occurred when the quenched solution was held for 30 min instead of conducting the analysis immediately. This observation proves that back exchange of functional groups on side chains was essentially complete and that back exchange of amide deuteriums was not significant during the time between quench and analysis [45].

To aid the interpretation of the H/D exchange results, we calculated, from the known Ca^{2+} binding constants, the binding fractions of the calcium-bound species of calmodulin, CaM–xCa ($x = 0-4$), as a function of total calcium concentration, Ca_T, at a total calmodulin concentration, CaM_T, of 15 μM. Owing to the complexity of the equations involved, no analytic solutions for calculating the binding fractions in terms of the total calcium concentration are possible. Therefore, we approached the problem indirectly by using the concentration of free Ca, $[Ca^{2+}]$, as an independent parametric variable from which the binding fractions and the corresponding total calcium concentration can be calculated. Let the sequential additions of Ca^{2+} to calmodulin be represented

$$\mathrm{CaM} - (x-1)\mathrm{Ca} + \mathrm{Ca}^{2+} \underset{\rightleftharpoons}{K_X} \mathrm{CaM}{-}x\mathrm{Ca}$$

$$K_x = [\mathrm{CaM}{-}x\mathrm{Ca}]/[\mathrm{CaM} - (x-1)\mathrm{Ca}] \cdot [\mathrm{Ca}^{2+}]$$

where $x = 1$–4 (1)

The K_x's are the sequential equilibrium binding constants: $K_1 = 1.3 \times 10^5\ M^{-1}$, $K_2 = 3.7 \times 10^5\ M^{-1}$, $K_3 = 3.2 \times 10^4\ M^{-1}$, and $K_4 = 3.2 \times 10^4\ M^{-1}$ [25]. Total concentrations of calmodulin and calcium, Ca_T, are given by:

$$\mathrm{CaM}_T = [\mathrm{CaM}] + [\mathrm{CaM}{-}\mathrm{Ca}] + [\mathrm{CaM}{-}2\mathrm{Ca}] + [\mathrm{CaM}{-}3\mathrm{Ca}] + [\mathrm{CaM}{-}4\mathrm{Ca}] \quad (2)$$

$$\mathrm{Ca}_T = [\mathrm{Ca}] + [\mathrm{CaM}{-}\mathrm{Ca}] + 2[\mathrm{CaM}{-}2\mathrm{Ca}] + 3[\mathrm{CaM}{-}3\mathrm{Ca}] + 4[\mathrm{CaM}{-}4\mathrm{Ca}] \quad (3)$$

By substituting the equilibrium equations to eliminate explicit reference to calcium-bound species, we obtain after algebraic manipulation:

$$CaM_T = [CaM]^*D \quad (4)$$

$$D = 1 + K_1[Ca^{2+}] + K_1K_2[Ca^{2+}]^2 + K_1K_2K_3[Ca^{2+}]^3 + K_1K_2K_3K_4[Ca^{2+}]^4 \quad (5)$$

$$Ca_T = [Ca^{2+}] + K_1[Ca^{2+}]CaM_T\{1 + K_2[Ca^{2+}] + K_2K_3[Ca^{2+}]^2 + K_2K_3K_4[Ca^{2+}]^3\}/D \quad (6)$$

We define the binding fractions for the calcium-bound species of calmodulin as $f_x = [CaM - xCa]/CaM_T$ for $x = 0-4$, which corresponds to the fraction of the calmodulin population having x Ca^{2+} bound. Upon elimination of the calcium-bound species, we obtain:

$$f_0 = 1/D \quad (7)$$

$$f_1 = K_1[Ca^{2+}]/D \quad (8)$$

$$f_2 = K_1K_2[Ca^{2+}]^2/D \quad (9)$$

$$f_3 = K_1K_2K_3[Ca^{2+}]^3/D \quad (10)$$

$$f_4 = K_1K_2K_3K_4[Ca^{2+}]^4/D \quad (11)$$

Thus, eqs 5–11 define the binding fractions, f_x, and the total calcium concentration, Ca_T, in terms of known equilibrium binding constants, the known total calmodulin concentration, CaM_T, and the free concentration of calcium, $[Ca^{2+}]$. We calculated a set of f_x's and Ca_T over a range of $[Ca^{2+}]$ from 10 nM to 0.10 M and plotted the f_x's with respect to Ca_T for $CaM_T = 15$ μM (Figure 2) from which we deduced the population of calcium-bound calmodulin species for a given total calcium concentration.

The extent of deuteration of the apo and the bound calmodulin was measured in a time-dependent manner, allowing us to construct a kinetic curve for the H/D exchange (Figure 3). Exchange kinetics were studied for apo and Ca^{2+}-loaded calmodulin at 0.04 and 0.49 mM Ca^{2+} concentrations. These two concentrations of calcium acetate (0.04 and 0.49 mM) were chosen because, according to the distribution of calcium-bound species, the dominant calmodulin forms at 0.04 and 0.49 mM Ca^{2+} are CaM-2Ca and CaM-4Ca, respectively.

The differences in the amount of deuterium incorporation between calcium-free and calcium-loaded calmodulin at 0.04 and 0.49 mM Ca^{2+} after 60 min of incubation in D_2O are 11 and 24 protons, respectively. After 4 h, the observed protein mass (and presumably the exchange) had become relatively constant; therefore, we present only the early part of the time dependency for exchange. When calmodulin interacts with 0.49 mM Ca^{2+} mM, the rate of exchange at times less than 60 min appears to be smaller than that when $[Ca^{2+}]$ is 0.04 mM, and the extent of exchange reaches a plateau after 1 h (Figure 3). The deuterium incorporation for the calmodulin when $[Ca^{2+}] = 0.49$ mM is lower than when $[Ca^{2+}] = 0.04$ mM and must result from new protection of exchangeable amide hydrogens, presumably because the calcium-loaded calmodulin assumes a more compact structure.

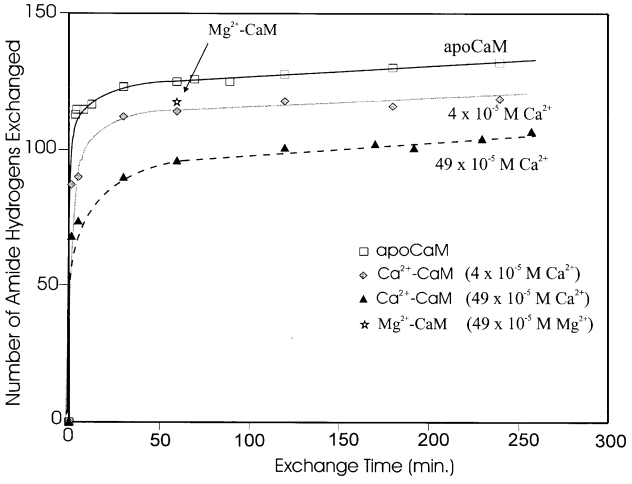

Figure 3. Time dependence for the H/D exchange of calmodulin, with and without added Ca^{2+}. The extent of H/D exchange at one time and for one concentration of Mg^{2+} is given as a reference. The solid and dashed lines are the best fits as judged by eye.

We then titrated calmodulin by varying the Ca^{2+} concentration from 0.01 mM to 1 mM and submitted the solution at discrete titration points to H/D exchange for a time at which the exchange was relatively constant (i.e., 60 min). When the concentration of calcium was low (e.g., 0.01 and 0.02 mM) and the apo form was the dominant species, there were no detectable changes in deuterium uptake (Figure 4). When the concentration of

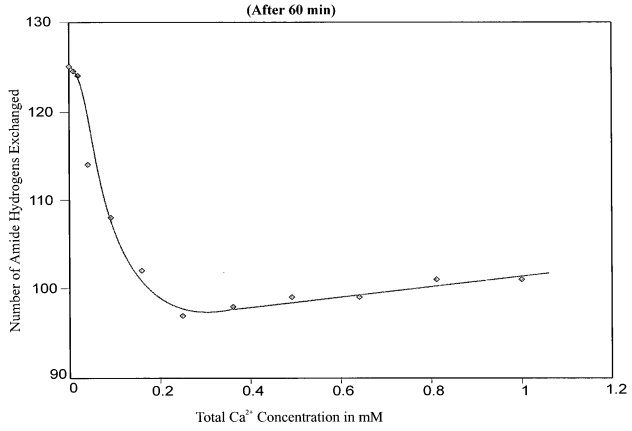

Figure 4. Ca^{2+} titration curve for the H/D exchange of calmodulin. Note the break at approximately 0.25 mM added Ca^{2+}. The concentration of calmodulin was 15 μM. The solid line is the best fit as judged by eye.

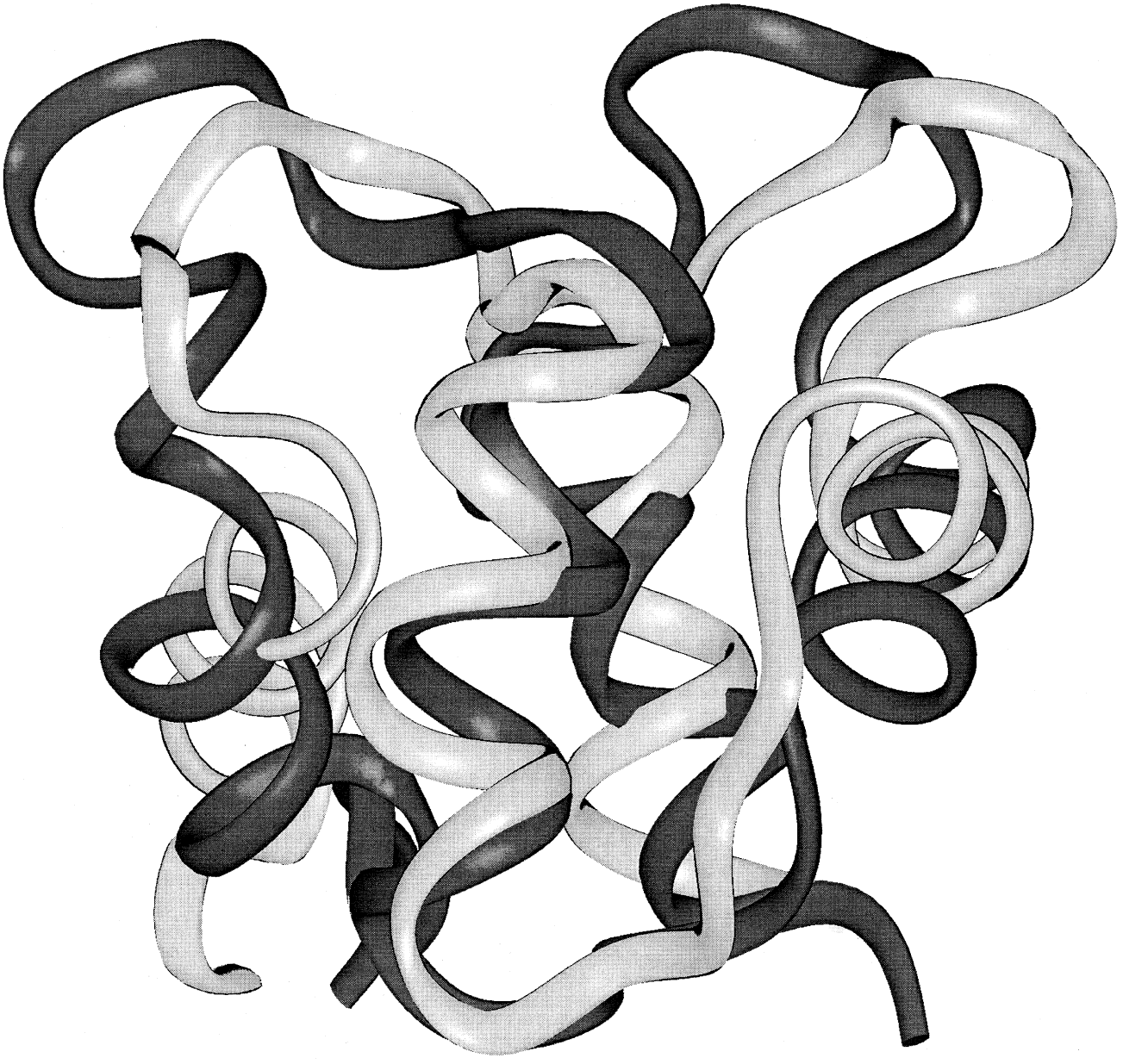

Figure 5. Ribbon structures of the apo (dark) and Ca^{2+}-ligated (light) calmodulins showing two of the four Ca-binding sites (top right and left). Structure coordinates are from [42] and were taken from the NCBI database (apo: 1CMF and Ca^{2+}-bound: 1CMG).

calcium became sufficiently large such that other Ca^{2+}-bound forms of calmodulin began to form, a decrease in deuterium incorporation occurred. At $[Ca^{2+}] = 0.25$ mM, the amount of deuterium that was incorporated reached a minimum (Figure 4). At this concentration, the CaM-4Ca is at least 85% of all forms of Ca^{2+}-bound calmodulin (compare Figures 2 and 4). Upon further increases in the calcium concentration (up to 1 mM), the extent of deuteration increased slowly, possibly owing to repulsion between excessive positive charge on the protein surface as nonspecific Ca^{2+} binding takes place, leading to a slight "reopening" of the structure (nonspecific binding can be seen with MS [28]).

We also used ESI to monitor H/D exchange experiments designed to reveal the structural changes of calmodulin triggered by binding to Mg^{2+}. The extent of deuterium incorporation in 0.49 mM Mg^{2+} changed only slightly from that of the apocalmodulin and is substantially greater than that in 0.49 mM Ca^{2+} (Figure 3). The much smaller decrease of H/D exchange in the presence of Mg^{2+} compared to that in the presence of Ca^{2+} indicates a less folded structure for Mg^{2+}-bound calmodulin. This smaller extent of folding of calmodulin upon addition of Mg^{2+} is consistent with the changes in CD and fluorescence spectra of calmodulin in the presence of Mg^{2+} and the interpretation that

magnesium primarily binds to N-terminal domain of calmodulin [46–48].

H/D Exchange of Lysozyme

To verify that the differences in H/D exchange are due to differences in protein higher order structure and not to changes in solution environment (e.g., changes in ionic strength as Ca^{2+} is added), we carried out control experiments with lysozyme. Lysozyme (14 kDa) is similar in size to calmodulin (17 kDa) and also binds Ca^{2+} and Mg^{2+} ions. According to NMR [49] and X-ray crystallography [50], the tertiary structures of apo and metal-bound lysozymes are nearly superimpossible, making them appropriate candidates for control experiments.

Addition of 0.49 mM Ca^{2+} to lysozyme led to the formation of various metal-loaded species. The most abundant metal-containing species formed upon ESI is Lys-Ca, whereas Lys-2Ca and Lys-3Ca also form but are less abundant.

We measured the extent of deuterium incorporation in apolysozyme and Ca^{2+}-bound lysozyme in a time-dependent manner. The differences in deuterium uptake between apo and Ca^{2+}-bound lysozyme are very small and remain nearly constant with time: differences of six and eight protons exchanged after 60 and 240 min of exchange, respectively. The exchange profiles as a function of the time range that we investigated were not significantly affected by binding of this protein to Ca^{2+}. The relatively small differences in H/D exchange for metal-free and metal-bound lysozyme are good evidence that changes in H/D exchange of calmodulin when titrated with Ca^{2+} do result from changes in its high order structure and not from some other unexpected effect.

Conclusion

The results of ESI-MS investigation of interaction of calmodulin with Ca^{2+} demonstrate that calmodulin adopts a tighter, less solvent-accessible structure as the protein binds with Ca^{2+}. The structural changes are revealed in Figure 5, which contains an overlay of approximately one half of the Ca^{2+}-ligated and the apocalmodulin structures. The main effect of Ca^{2+} binding is seen by comparing the apo (darker) structure) with the bound structure. In the apo structure, the two Ca^{2+} binding loops (on the upper right and left portions of the figure) are located behind the plane of the figure. They move forward upon ligation to Ca^{2+}, causing the α-helices to become tighter and presumably less accessible to water. Thus, the extent of H/D exchange decreases as the protein takes up Ca^{2+}. It is that tighter structure that binds with proteins, peptides, and other small molecules. Addition of Mg^{2+} to calmodulin, on the other hand, does not cause any significant change in the tertiary structure of the protein.

If the binding constants for Ca^{2+} and calmodulin were not known, the end point in the titration may be a convenient means of calculating an overall binding constant. This may be a general outcome of a mass spectrometry method that is applied to metal binding to proteins.

Acknowledgments

The research was supported by the National Centers for Research Resources of the NIH (grant no. P41RR00954). The authors are grateful to Professor David Cistola for helpful discussions and to Robert Latek and Professor E. Unanue for help in obtaining the structures for Figure 5.

References

1. Snyder, A. P., Ed. *Biochem. Biotechnol. Appl. Electrospray Ionization Mass Spectrom., ACS Symp. Ser.* **1996,** *619*.
2. Schnier, P. D.; Gross, D. S.; Williams, E. R. *J. Am. Soc. Mass Spectrom.* **1995,** *6*, 1086–1097.
3. Smith, R. D.; Loo, J. A.; Edmonds, C. G.; Barinaga, C. J.; Udseth, H. R. *Anal. Chem.* **1990,** *62*, 882–899.
4. Covey, T. R.; Bonner, R. F.; Shushan, B. I.; Henion, *J. Rapid Commun. Mass Spectrom.* **1988,** *2*, 249–256.
5. Katta, V.; Chait, B. T. *Rapid Commun. Mass Spectrom.* **1991,** *5*, 214–217.
6. LeBlanc, J. C. Y.; Beuchemin, D.; Siu, K. W. M.; Guevremont, R.; Berman, S. S. *Org. Mass Spectrom.* **1991,** *26*, 831–839.
7. Chowdury, S. K.; Cohen, S.; Chait, B. T. *J. Am. Chem. Soc.* **1990,** *112*, 9012–9013.
8. Mirza, U.; Cohen, S.; Chait, B. T. *Anal. Chem.* **1993,** *65*, 1–6.
9. Miranker, A.; Robinson, C. V.; Radford, S. E.; Aplin, R. T.; Dobson, C. M. *Science* **1993,** *262*, 896–900.
10. Robinson, C. V.; Gross, M.; Eyles, S. J.; Ewbank, J. J.; Mayhew, M.; Hartl, F. U.; Dobson, C. M.; Radford, S. E. *Nature* **1994,** *372*, 646–651.
11. Wagner, D. S.; Anderegg, R. J. *Anal. Chem.* **1994,** *66*, 706–711.
12. Wagner, D. S.; Melton, L. G.; Yan, Y. B.; Erickson, B. W.; Anderegg, R. *J. Prot. Sci.* **1994,** *3*, 1305–1314.
13. Katta, V.; Chait, B. T. *J. Am. Chem. Soc.* **1993,** *115*, 6317–6321.
14. Englander, S. W.; Kallenbach, N. R. *Q. Rev. Biophys.* **1984,** *16*, 521–655.
15. Englander, J. J., Rogero, J. R.; Englander, S. W. *Anal. Biochem.* **1985,** *147*, 234–244.
16. Baldwin, R. L. *Trends Biochem. Sci. (Pers. Ed.)* **1989,** *14*, 291–294.
17. Baldwin, R. L. *J. Biomol. NMR* **1995,** *5*, 103–109.
18. Zhang, Z.; Smith, D. L. *Protein Sci.* **1993,** *2*, 522–531.
19. Liu, Y.; Smith, D. L. *J. Am. Soc. Mass Spectrom.* **1994,** *5*, 19–28.
20. Zhang, Z.; Smith, D. L. *Protein Sci.* **1996,** *5*, 1282–1289.
21. Mills, J. J.; Bailey, B. L.; Johnson, J. D. *Biochemistry* **1985,** *24*, 4897–4902.
22. O'Neill, K. T.; DeGrado, W. F. *Proc. Nat. Acad. Sci. USA* **1985,** *82*, 4954–4958.
23. Creenlee, D. V.; Andreasen, T. J.; Storm, D. R. *Biochemistry* **1982,** *21*, 2759–2764.
24. Barbato, G.; Ikura, M.; Kay, L. E.; Pastor, R. W.; Bax, A. *Biochemistry* **1992,** *31*, 5269–5278.
25. Kuboniwa, H.; Tjandra, N.; Grzesiek, S.; Ren, H.; Klee, C. B., Bax, A. *Nature Struct. Biol.* **1995,** *2*, 768–776.
26. Finn, B. E.; Evenäs, J.; Drakenberg, T.; Waltho, J. P.; Thulin, E.; Forsén, S. *Nature Struct. Biol.* **1995,** *2*, 777–783.
27. Zhang, M.; Tanaka, T.; Ikura, M. *Nature Struct. Biol.* **1995,** *2*, 758–767.
28. Nemirovskiy, O.; Ramanathan, R.; Gross, M. L. *J. Am. Soc. Mass Spectrom.* **1997,** *8*, 809–812.

29. Babu, Y. S.; Bugg, C. E.; Cook, W. J. *J. Mol. Biol.* **1988,** *204*, 191–204.
30. Taylor, D. A.; Sack, J. S.; Maune, J. F.; Beckingham, K.; Quiocho, F. A. *J. Biol. Chem.* **1991,** *266*, 21375–21380.
31. Chattopadhyaya, R.; Meador, W. E.; Means, A. R.; Quiocho, F. A. *J. Mol. Biol.* **1992,** *228*, 1177–1192.
32. Heidorn, D. B.; Trewhella, J. *Biochemistry* **1988,** *27*, 909–915.
33. Yoshino, H.; Wakita, M.; Izumi, Y. *J. Biol. Chem.* **1993,** *268*, 12123–12128.
34. Seamon, K. B. *Biochemistry* **1980,** *19*, 207–215.
35. Ikura, M.; Hiraoki, T.; Hikichi, K.; Mikuni, T.; Yazawa, M.; Yagi, K. *Biochemistry* **1983,** *22*, 2573–2579.
36. Ikura, M.; Hiraoki, T.; Hikichi, K.; Minova, O.; Yamaguchi, H.; Yazawa, M.; Yagi, K. *Biochemistry* **1984,** *23*, 3124–3128.
37. Ikura, M.; Minova, O.; Hikichi, K. *Biochemistry* **1985,** *24*, 4264–4269.
38. Ikura, M.; Spera, S.; Barbato, G.; Kay, L. E.; Krinks, M.; Bax, A. *Biochemistry* **1991,** *30*, 9216–9228.
39. Hoffman, R. C.; Klevit, R. E. In *Techniques in Protein Chemistry II*; Villafranca, J., Ed.; Academic: San Diego, 1991; pp 383–391.
40. Dedman, J. R.; Potter, J. D.; Jackson, R. L.; Johnson, J. D.; Means, A. *J. Biol. Chem.* **1977,** *252*, 8415–8422.
41. Crouch, T. H.; Klee, C. B. *Biochemistry* **1980,** *19*, 3692–3698.
42. Sorensen, B. R.; Shea, M. A. *Biophys. J.* **1996,** *71*, 3407–3420.
43. Yao, Y.; Schöneich, C.; Squier, T. C. *Biochemistry* **1994,** *33*, 7797–7810.
44. Gross, M. L. Tandem mass spectrometry: Multisector magnetic instruments. In *Methods in Enzymology, Vol 193, Mass Spectrometry*; McCloskey, J. A., Ed.; Academic: San Diego, 1990; pp 131–153.
45. Englander, J. J.; Calhoun, D. B.; Englander, S W. *Anal. Biochem.* **1979,** *92*, 517–524.
46. Forsen, S.; Vogel, H. J.; Drakenberg, T. In *Calcium and Cell Function*; Cheung, Ed.; Academic: New York, 1986; Vol. 6, pp 113–157.
47. Iida, S.; Potter, J. D. *J. Biochem.* **1986,** *99*, 1765.
48. Milos, M.; Schaer, J. J.; Comte, M.; Cox, J. A. *Biochemistry* **1986,** *25*, 6279–6287.
49. Tsuge, H.; Koseki, K.; Miyano, M.; Shimazaki, K.; Chuman, T.; Matsomoto, T.; Noma, M.; Nitta, K.; Sugai, S. *Biochim. Biophys. Acta* **1991,** *1078*, 77–84.
50. Inaka, K.; Kuroki, R.; Kikuchi, M.; Matsushima, M. *J. Biol. Chem.* **1991,** *266*, 20666–20671.